DOI: 10.1002/ejic.200800046

# Organometallic Access to Intermetallic $\theta$-$CuE_2$ (E = Al, Ga) and $Cu_{1-x}Al_x$ Phases

Mirza Cokoja,[a] Balaji R. Jagirdar,[b] Harish Parala,[a] Alexander Birkner,[c] and Roland A. Fischer*[a]

**Keywords:** Alloys / Intermetallic phases / Copper / Aluminum / Nanotechnology

In this work, we compare different precursor approaches for the mild decomposition to copper–aluminum and –gallium powder materials in nonaqueous solution. Referring to previous work on the preparation of Cu–Al alloy materials from [$(AlCp^*)_4$] and [CpCu($PMe_3$)], the amine-stabilized metal trihydrides [$(Me_3N)AlH_3$] and [(quinuclidine)$GaH_3$] were used as alternative sources for Al and Ga. In a comparative study, [$(Me_3N)AlH_3$] and [$(AlCp^*)_4$] were treated with the Cu precursors [CpCu($PMe_3$)] and [{Cu(mesityl)}$_5$] in mesitylene solution in various molar ratios at 150 °C and 3 bar $H_2$ to give metallic precipitates of the composition $Cu_{1-x}Al_x$ (x = 0.67, 0.50, 0.31). Whereas the combination [$(AlCp^*)_4$] with [{Cu(mesityl)}$_5$] did not yield an intermetallic phase, all other Cu/Al precursor combinations led to alloyed Cu–Al materials. For x = 0.67, the $\theta$-$CuAl_2$ phase formed, as shown by X-ray powder diffraction (XRD) and solid-state magic-angle-spinning (MAS)NMR spectroscopic studies. Similarly, the reaction of [{Cu(mesityl)}$_5$] with [(quinuclidine)$GaH_3$] immediately led to the precipitation of a gray powder, without the addition of hydrogen. The powder was identified by means of XRD as $\theta$-$CuGa_2$. At x = 0.50 and below, the reactions were less phase selective depending on the precursor combination. [CpCu($PMe_3$)] combined with both Al precursors afforded a mixture of several Cu–Al phases, whereas [{Cu(mesityl)}$_5$] was treated with [$(Me_3N)AlH_3$] to yield a material whose X-ray signature was assigned to the monoclinic $Cu_{0.51}Al_{0.49}$ phase. The $\gamma$-$Cu_9Al_4$ phase could not be obtained from [CpCu($PMe_3$)]; instead, solid solutions of α-Cu were obtained. The treatment of [{Cu(mesityl)}$_5$] with [$(Me_3N)AlH_3$] in the Cu/Al molar ratio of 9:4 (x = 0.31) gave a gray powder, which could be identified by XRD as $\gamma$-$Cu_9Al_4$.



## Introduction

The synthesis of high-quality crystalline intermetallic phases by relatively simple and reproducible approaches is of both fundamental and technological interest, and we have been studying related chemical precursor strategies since a number of years.[1] In this regard, the classical Hume–Rothery phases, such as Cu–Al alloys, have attracted attention from the viewpoint of the understanding of chemical bonding and their importance as engineering materials.[2] The phase diagram of the binary Cu–Al system, which is one of the well-investigated cases,[3] shows several equilibrium intermediates such as β-$Cu_3Al$, $\gamma$-$Cu_9Al_4$, $Cu_4Al_3$, CuAl, and $\theta$-$CuAl_2$.[4] From examination of the Cu-rich side of the phase diagram between α-Cu and the $\theta$-$CuAl_2$ phases, it is obvious that it is very difficult to obtain a phase-pure copper aluminum intermetallic compound $Cu_{1-x}Al_x$ ($0.25 \leq x \leq 0.50$). To date, several processes to obtain $Cu_{1-x}Al_x$ alloys, including high-temperature melting are known. For example, Havinga et al. reported on the arc-melting synthesis of the $\theta$-$CuAl_2$ phase and characterized the compound by powder X-ray diffraction.[5] Recently, Grin et al. presented a full structural characterization of the $\theta$-$CuAl_2$ phase by single-crystal X-ray structural analysis (Figure 1) and detailed solid-state $^{63,65}$Cu NMR spectroscopy.[6,7]

El-Boragy et al. synthesized the hexagonal $Cu_{0.58}Al_{0.42}$ phase as well as the monoclinic $Cu_{0.51}Al_{0.49}$ phase by heat treatment.[8] Gulay and Harbrecht investigated the phase changes in α-CuAl structures, for example, the orthorhombic $\zeta_1$- and $\zeta_2$-$Cu_4Al_3$ phases.[9] These authors showed that the phase transformations take place at low temperatures; for example, the $\zeta_2$-$Cu_3Al_{4-\delta}$ phase decomposes to $\eta_2$-CuAl and $\zeta_1$-$Cu_4Al_3$ above 400 °C.[10] Other metallurgical methods include mechanical mixing of the Cu and Al metals. For instance, the formation of $\theta$-$CuAl_2$ and $\gamma$-$Cu_9Al_4$ were observed by ball milling, rolling, or welding tech-

[a] Lehrstuhl für Anorganische Chemie II – Organometallics & Materials, Ruhr-Universität Bochum,
Universitätsstraße 150, 44780 Bochum, Germany
Fax: +49-234-32-14174
E-mail: roland.fischer@ruhr-uni-bochum.de
[b] Department of Inorganic and Physical Chemistry, Indian Institute of Science,
Bangalore 560012, India
[c] Lehrstuhl für Physikalische Chemie I, Ruhr-Universität Bochum
44780 Bochum, Germany

Supporting information for this article is available on the WWW under http://www.eurjic.org or from the author.

   

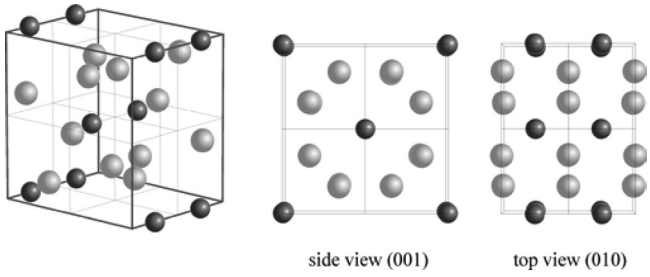


Figure 1. Elementary cell of the intermetallic *bct* $\theta$-$CuAl_2$ phase (left, Cu: dark gray, Al: light gray) and views at the (001) lattice plane (middle) and at the (010) plane (right). Structural data are taken from ref.[6]

niques[11–16] and certain thin film or interfacial reactions.[17,18] The solid-state reaction between Al and Cu powders during high-energy ball milling revealed the formation of only $\gamma$-$Cu_9Al_4$ for the composition $Cu_{1-x}Al_x$ ($0.3 \leq x \leq 0.7$). Obviously, this particular phase exhibits the largest driving force under such conditions.[11] Interfacial reactions of copper and aluminum multilayer films, however, lead to the formation of the $\theta$-$CuAl_2$ phase even with an excess amount of Cu.[17,18]

With an increase in the sintering time and/or temperature, the $\gamma$-$Cu_9Al_4$ phase is formed. However, in solid-state reactions between Cu and Al during mechanical alloying and heat treatment, it was found that $\gamma$-$Cu_9Al_4$ or $\theta$-$CuAl_2$ is formed as the first phase, depending on the molar ratios of the starting materials taken and the reaction conditions.[14] Several groups have shown that the situation in the Cu-rich $\gamma$-CuAl phase region is even more intricate.[19] The complex interplay of thermodynamic and kinetic factors during the low-temperature annealing of thin films leads to a sequential formation of metastable and equilibrium intermetallic compounds at the interfaces.[20]

The common factors of the synthetic methodologies summarized above are comparably high-energy solid-state and/or interfacial reactions. In contrast to this, the development of so-called soft-chemical molecular precursor routes to access metal and bimetallic alloy nanoparticles in solution has been attracting widespread interest in recent years.[21] We reported on soft-chemical approaches to colloidal intermetallic $Cu_{1-x}Al_x$ and $Cu_{1-x}Zn_x$ materials in particular aiming at free-standing alloy nanoparticles by hydrogenolysis of suitable organometallic precursors being stabilized as colloids.[22,23] Phase-pure $\theta$-$CuAl_2$ powder material was obtained by cohydrogenolysis of the precursors [CpCu($PMe_3$)] and [(AlCp*)$_4$] in mesitylene solution. Although [(AlCp*)$_4$] is a good source for the Al component, the difficulty in the synthesis of this particular precursor on a large scale is a drawback. In addition, the use of [CpCu($PMe_3$)] as a Cu precursor leads to phosphane-containing byproducts that are not easy to remove from the final alloy product. Other Cu precursors such as [Cu(OR)$_2$] [R = $CH(CH_3)CH_2N(CH_3)_2$][24] also cause problems due to noninnocent byproducts (i.e., alcohols, aldehydes, ketones) that react with the Al sources.

In our search for optimized precursor combinations for a wet chemical synthesis of metal aluminum and gallium alloys and intermetallic compounds we selected the alkylamine adduct stabilized trihydrides [($Me_3N$)$AlH_3$] and [(quinuclidine)$GaH_3$] as Al and Ga sources. The alane compound is a well-known starting material for the chemical vapor deposition (CVD) of thin Al films,[25] yet it is very reactive and even hazardous. Buhro et al. showed that this compound decomposes to $Al^0$ by thermolysis in organic solution with the gaseous byproducts $H_2$ and $NMe_3$.[26] It is well established that metal hydrides and anionic hydride complexes, such as Bogdanović's $MgH_2$[27] or $LiAlH_4$,[28–30] serve as precursors for the precursor synthesis of metal alloys. Accordingly, we recently showed that [($Me_3N$)$AlH_3$] and [Ni(cod)$_2$] (cod = *cis*,*cis*-1,5-cyclooctadiene) rapidly react to afford NiAl nanoparticles under hydrogen pressure.[31] Following this line and in order to avoid undesired phosphane byproducts, as in the case of the [CpCu($PMe_3$)] precursor, we chose the all-hydrocarbon and thus heteroatom-free [{Cu(mesityl)}$_5$] as an alternative precursor for Cu.[32] Boyle et al. reported that thermolysis of this compound at 300 °C in hot hexadecylamine (HDA) gives Cu colloids of a very narrow size regime.[33] The obvious advantage of this precursor compared to [CpCu($PMe_3$)] is the likely conversion of the organic ligand into mesitylene as a very innocent leaving group upon hydrogenolysis. Below we report our results by using the precursor concept outlined above in order to derive a versatile wet chemical synthesis of Cu/Al and Cu/Ga alloys and compounds.

## Results and Discussion

### Hydrogenolysis of [{Cu(mesityl)}$_5$] to Yield Cu

The hydrogenolysis of [{Cu(mesityl)}$_5$] alone under the typical conditions of soft-chemical Cu–Al alloy formation was studied first. The treatment of a mesitylene solution of [{Cu(mesityl)}$_5$] with hydrogen (3 bar) at 150 °C leads to the formation of metallic copper grains that are 0.5–1 mm in diameter (Scheme 1). According to elemental analysis, the Cu content is 99 wt.-%, with trace amounts of C and H as the only other elements present. $^1$H NMR spectroscopic and GC–MS analysis of the colorless supernatant evidenced no other byproducts than mesitylene, which suggests a clean reaction, as expected.

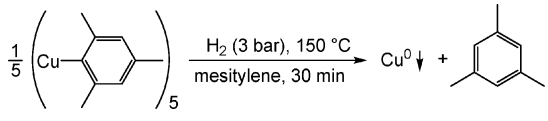


Scheme 1. Quantitative decomposition of [{Cu(mesityl)}$_5$] to Cu powder under hydrogen pressure in mesitylene solution.

The X-ray powder diffraction pattern (Figure 2) of the shiny metallic copper grains matches that of the copper reflection pattern (JCPDS No. 4-0836), which exhibits sharp reflections. Interestingly, the intensity ratios of the 220 (56%), 311 (79%), and 222 (31%) reflections to the strong-

  

est (111) reflection significantly deviate from literature data for bulk Cu (220: 20%, 311: 17%, 222: 5%), which points to anisotropic particles. However, some movement of copper grains inside the capillary during the measurement cannot be ruled out, which contributes to this deviation in the intensity ratios. The average primary crystallite size was estimated to be $25 \pm 5$ nm by using the Scherrer equation. Hence, [{Cu(mesityl)}$_5$] can be employed as a precursor for Cu-containing nanoparticles by the "chimie douce" approach, established by B. Chaudret.[34]

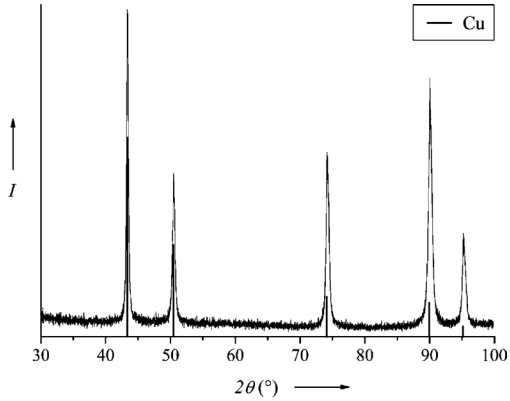


Figure 2. XRD pattern of the Cu powder obtained by decomposition of [{Cu(mesityl)}$_5$] under 3 bar $H_2$ pressure/150 °C in mesitylene.

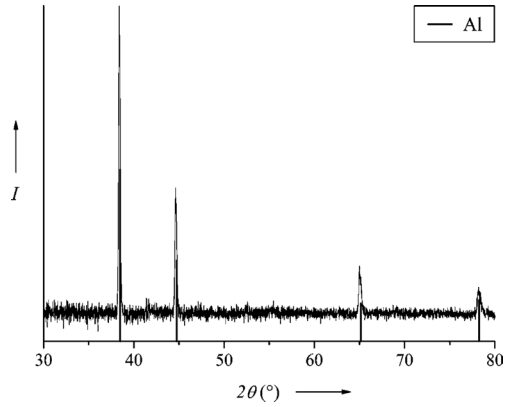


Figure 3. XRD pattern of Al powder from the decomposition of [$(Me_3N)AlH_3$] under 3 bar $H_2$/150 °C in mesitylene (Al reference taken from the JCPDA database, No. 4-787).

### Hydrogenolysis of [$(Me_3N)AlH_3$] to Al Powder

The compound [$(Me_3N)AlH_3$] quantitatively decomposes to elemental aluminum in mesitylene under 3 bar $H_2$ at 150 °C within 1 h, whereas [$(AlCp^*)_4$] decomposes after only 15 min under the same conditions. Workup of the reaction mixture afforded a highly pyrophoric powder. The XRD pattern evidences the presence of $Al^0$ (Figure 3). The Al reflections are sharper in comparison to those of Al obtained from [$(AlCp^*)_4$].[22a] The average diameter of the crystalline domains is calculated to be around 50 nm, which is in quite good agreement with the results of Buhro.[26b] It is likely that the decomposition of [$(Me_3N)AlH_3$] is induced purely thermally. It has been reported that heating of [$(Me_3N)AlH_3$] above 100 °C in the solid state gives $NMe_3$ and polymeric $[AlH_3]_x$, which further decomposes to $Al^0$ and $H_2$.[35] The solid-state $^{27}Al$ MAS NMR spectrum (see Supporting Information) exhibits a Knight shift at $\delta$ = 1640 ppm, which is assignable to $Al^0$ and in agreement with our previous work by using [$(AlCp^*)_4$] as a precursor[22a] and the data of Al powder reported in the literature.[36] Two signals for $Al_2O_3$ are observed at $\delta$ = 56 and 1 ppm, depending on the nature of the coordination geometry of the $AlO_x$ species.[37] In order to detect the fate of the amine ligand, the reaction was followed by NMR spectroscopy (decomposition in a pressure-stable NMR tube in [$D_{12}$]-mesitylene). The $^1H$ NMR spectrum of the precursor [$(Me_3N)AlH_3$] shows a broad signal at $\delta$ = 3.81 ppm, which is assignable to the Al–H atoms, and a sharp singlet at $\delta$ = 1.93 ppm for the hydrogen atoms of the coordinated $NMe_3$ molecule. The corresponding $^{27}Al$ NMR spectrum exhibits a broad resonance at $\delta$ = 136 ppm for the starting material. The $^1H$ NMR spectrum recorded after treatment with 3 bar $H_2$ at 150 °C for 24 h does not exhibit the hydride signals, whereas the signal for the $NMe_3$ moiety shifts to 2.10 ppm (free amine). Further, a weak signal of $H_2$ at $\delta$ = 4.61 ppm is observed. The $^{27}Al$ NMR spectrum evidences the disappearance of the starting material. In addition, no Al-containing species are noted, which is indicative of quantitative decomposition of [$(Me_3N)AlH_3$].

### Formation of the $\theta$-$CuAl_2$ Phase

Previously, we showed that [$CpCu(PMe_3)$] (1 equiv.) and [$(AlCp^*)_4$] (0.5 equiv.) quantitatively yields the intermetallic phase $\theta$-$CuAl_2$.[22a] However, this synthesis suffers from certain problems, as outlined in the introduction section (also see Supporting Information). By using these precursors, it was not possible to synthesize other phase-pure Cu-rich phases, such as $Cu_{0.50}Al_{0.50}$ or $\gamma$-$Cu_9Al_4$; rather, a mixture of several α-Cu/Al phases was obtained (vide infra). The analogous cohydrogenolysis of [{Cu(mesityl)}$_5$] with [$(AlCp^*)_4$] did not result in the alloying to any Cu–Al phase. Hence, we substituted [$(AlCp^*)_4$] against [$(Me_3N)$-$AlH_3$] and examined the reactivity of this Al precursor with [$CpCu(PMe_3)$] and with the alternative Cu source [{Cu(mesityl)}$_5$] for comparison.

### Reaction of [$(Me_3N)AlH_3$] with [$CpCu(PMe_3)$]

Addition of a mesitylene solution of [$(Me_3N)AlH_3$] (2 equiv.) to a mesitylene solution of freshly sublimed [$CpCu(PMe_3)$] (1 equiv.) in a Fischer–Porter bottle resulted in a color change from bright yellow to orange and finally dark red. Soon after (<30 s), a grayish powder precipitated, accompanied by vigorous gas evolution. In order to complete the reaction, the solution was then set to 3 bar $H_2$, heated to 150 °C, and stirred for 24 h. The residue was isolated and washed first with 1,4-dioxane to remove residual

  

phosphane and phosphane oxide byproducts and thereafter with *n*-pentane, and it was then dried in vacuo at room temperature.

In order to characterize the byproducts, the same reaction was carried out in a pressure-stable sealed NMR tube (in the presence of 4 bar $H_2$). In the $^1H$ NMR spectrum after 1 d of reaction time, the signals of cyclopentadiene (CpH) at $\delta$ = 6.49, 6.32, and 2.75 ppm and free $PMe_3$ ($\delta$ = 0.82 ppm) and $NMe_3$ ($\delta$ = 2.11 ppm) were found, which is indicative of full decomposition of both precursors without any undesired side reactions. Accordingly, in the $^{31}P$ NMR spectrum, only the signal of $PMe_3$ was found at $\delta$ = –62.2 ppm. The $^{27}Al$ NMR spectrum did not exhibit any signals. The X-ray diffractogram (Figure 4a) of the isolated powder as described above clearly exhibits the characteristic reflections of the $\theta$-$CuAl_2$ phase (body-centered tetragonal *I*4/*m*cm, JCPDS No. 25-0012). There was no indication of the presence of either pure Cu or Al or of another Cu–Al phase, which would certainly be crystalline under the conditions described (vide supra). The average crystallite domain size was estimated to be around 75 nm by using the Scherrer equation. The results of elemental analysis match the expected molar ratio of Cu and Al (see Experimental Section); however, the total metal content of the sample was not 100%. In all Cu/Al samples described in this work, the residual content is C, H, and O, which stems from oxidation and hydrocarbon artifacts (solvent and/or decomposition products) that are not fully desorbed from the particle surface. The $^{27}Al$ MAS NMR of the sample (diluted with $SiO_2$ powder) reveals a strong signal at $\delta$ = 1492 ppm (Figure 5a), which is assignable to the Al Knight shift in $\theta$-$CuAl_2$ in the range of 1480[38] to 1500[7] and 1530 ppm[39] and thus in agreement with the literature. A strong signal of $Al_2O_3$[37] at $\delta$ = 31.3 ppm is visible, which is indicative of partial oxidation of the sample (see Supporting Information). The co-

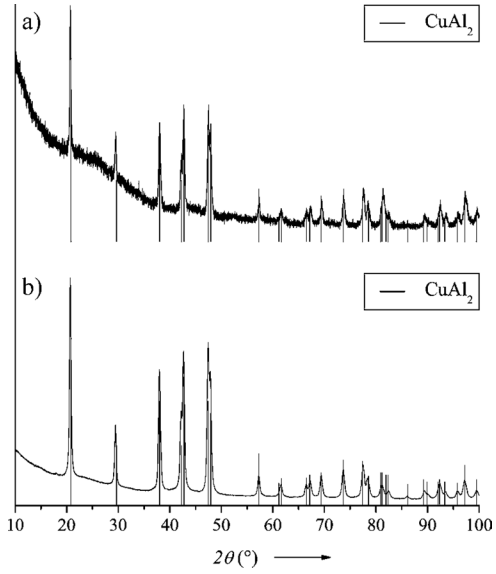


Figure 4. XRD diagrams of $\theta$-$CuAl_2$, synthesized from (a) 0.5 equiv. [$CpCu(PMe_3)$] and (b) 0.1 equiv. [{$Cu(mesityl)\}_5$] with 1 equiv. [$(Me_3N)AlH_3$] under $H_2$ pressure.

hydrogenolysis of the precursors according to Scheme 2 was carried out in the absence of a surfactant; therefore, agglomeration of the resulting particles could not be avoided. As evidenced by the TEM images, the agglomerated par-

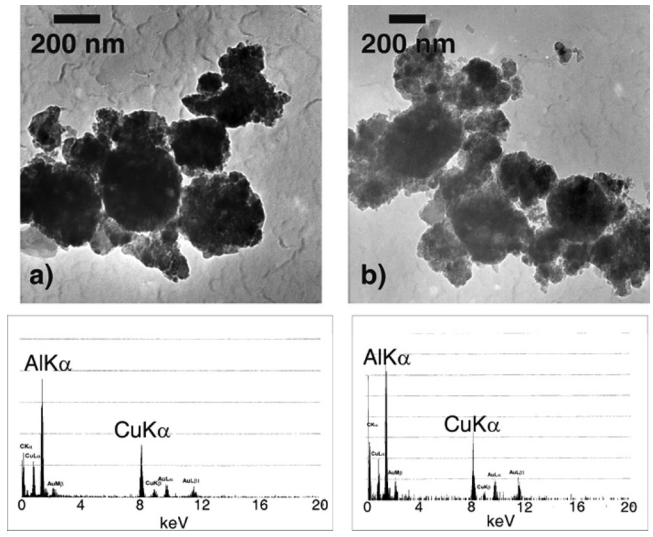


Figure 5. TEM images of $\theta$-$CuAl_2$ powders (top), synthesized by cohydrogenolysis of (a) [$CpCu(PMe_3)$] and 2 equiv. of [$(Me_3N)AlH_3$] and (b) 0.2 equiv. of [{$Cu(mesityl)\}_5$] and 2 equiv. of [$(Me_3N)AlH_3$], and the corresponding EDX analyses (bottom).

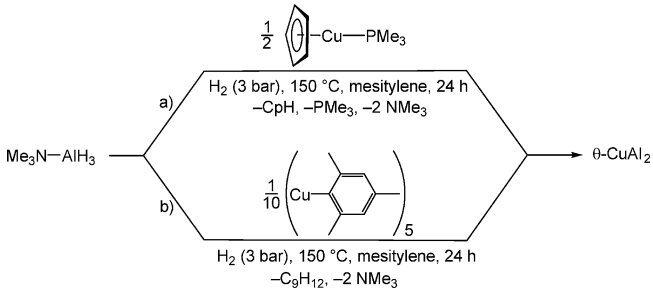


Scheme 2. Synthesis of the $\theta$-$CuAl_2$ powder from cohydrogenolysis of (a) [$CpCu(PMe_3)$] and (b) [{$Cu(mesityl)\}_5$] with [$(Me_3N)AlH_3$].

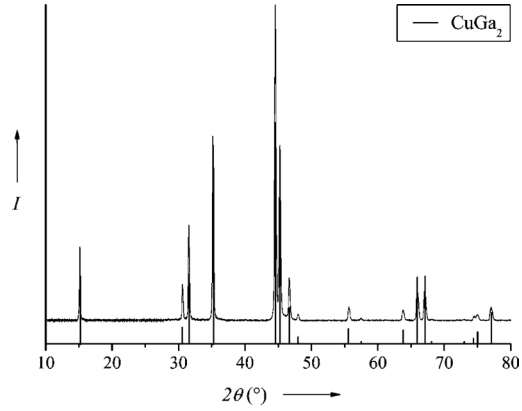


Figure 6. XRD diagram of the $\theta$-$CuGa_2$ powder (JCPDS No. 25-0275) obtained by cohydrogenolysis of [{$Cu(mesityl)\}_5$] and [(quinuclidine) $GaH_3$].

  

ticles exhibit a wide size distribution of 100–200 nm (Figure 5a, top left). The EDX analysis of a selected area (Figure 6a, bottom left) reveals an atomic Cu/Al ratio of around 1.0:2.1 (±10%). Analysis performed on several different particles does not indicate any Cu-rich, Al-, or Cu-only regions.

### Reaction of [(Me$_3$N)AlH$_3$] with [{Cu(mesityl)}$_5$]

The treatment of a mesitylene solution of the alternative Cu precursor [{Cu(mesityl)}$_5$] (1 equiv.) with a mesitylene solution of [(Me$_3$N)AlH$_3$] (10 equiv.) gave a red-brown solution, which was then set to 3 bar $H_2$ and heated to 150 °C. Within a few minutes, a gray, metallic shiny precipitate formed. Workup of the reaction mixture afforded a gray powder in quantitative yield, which suggests complete decomposition of both precursors (Scheme 2). According to elemental analysis (AAS), the Cu/Al ratio of the isolated powder (after workup as described before) is 1.00:2.11 and almost matched the expected Cu/Al ratio of 1:2. The $^1$H NMR spectroscopic and GC–MS studies do not provide any insight into the fate of the mesityl group that would have resulted upon decomposition of [{Cu(mesityl)}$_5$] to Cu$^0$. A reaction in a pressure-stable NMR tube was carried out to trace the fate of the mesityl group and to further characterize the mechanism of decomposition. The initial $^1$H NMR spectrum of [{Cu(mesityl)}$_5$] (see Supporting Information) shows two sets of signals of the pentameric cluster [{Cu(mesityl)}$_5$] at $\delta$ = 6.64 ppm (ring-H, 3 H), 2.96 (*ortho*-CH$_3$, 6 H), and 2.02 ppm (*para*-CH$_3$, 3 H), which is in equilibrium with the dimeric species [{Cu(mesityl)}$_2$] ($\delta$ = 6.56, 2.90, and 1.93 ppm) as reported in the literature.[32] After addition of [(Me$_3$N)AlH$_3$] and subsequent decomposition at 4 bar $H_2$ and 150 °C for 24 h, the $^1$H NMR spectrum is comprised of only one singlet due to free trimethylamine at $\delta$ = 2.11 ppm, which also suggests full decomposition of [(Me$_3$N)AlH$_3$]. The expected signals of the other byproduct, mesitylene, overlap the signals of residual protons of [D$_{12}$]mesitylene and thus could not be integrated. The $^{27}$Al NMR spectrum of the solution does not exhibit any signals. The initial signal of the alane complex at $\delta$ = 136 ppm, however, disappears so that undesired side reactions (e.g., to Al$^{III}$ complexes), which would lower the yield of Al$^0$, can be ruled out. The X-ray diffraction pattern of the synthesized sample (Figure 4b) clearly exhibits all reflections of the $\theta$-CuAl$_2$ phase (khatyrkite, body-centered tetragonal *I*4/*m*cm, JCPDS No. 25-0012). The reflections appear to be slightly broadened in comparison to the X-ray diffraction patterns of the $\theta$-CuAl$_2$ sample, which was prepared from [CpCu(PMe$_3$)] and from [(AlCp*)$_4$],[22a] or from [(Me$_3$N)AlH$_3$] (Figure 4a), respectively. The average size of the crystalline domains in the particle grains was calculated to be 25 ± 5 nm by using the Scherrer equation. In the $^{27}$Al MAS NMR spectrum of the powder, the Knight shift of Al at $\delta$ = 1494 ppm is observed, which is in good agreement with the previously published data for $\theta$-CuAl$_2$.[7,38,39] The TEM image of the sample, which was suspended in toluene upon sonication, exhibits strongly agglomerated particles (Figure 5b), similar to the $\theta$-CuAl$_2$ particles synthesized from [CpCu(PMe$_3$)] and [(Me$_3$N)-AlH$_3$]. The EDX analysis of several selected particle regions confirmed the expected molar Cu/Al ratio of 1:2 (±10%).

### Formation of the $\theta$-CuGa$_2$ Phase

The Cu–Ga phase diagram[4a] is quite similar to that of Cu–Al, with several Cu-rich phases ($\gamma_{1,2,3}$-Cu$_3$Ga$_{1-x}$, β-Cu$_3$Ga, ζ-Cu$_4$Ga$_{1-x}$), as well as the Ga-rich $\theta$-CuGa$_2$ phase. Taking into account the intricacy of phase purity and possible phase transformations, as in the case of α-CuAl phases, the $\theta$-CuGa$_2$ phase was selected as a synthetic target. In contrast to [(R$_3$N)AlH$_3$] compounds, the corresponding alkylamine adduct stabilized gallium trihydride species are less stable and difficult to handle. An exception is [(quinuclidine)GaH$_3$] (quinuclidine = 1-azabicyclo[2.2.2]-octane), which is thermally stable as a microcrystalline powder up to 80 °C and stable for weeks in solution under treatment with 3 bar $H_2$ and 150 °C. However, thermolysis of a mesitylene solution at 150 °C in the absence of $H_2$ leads to rapid decomposition to Ga$^0$. This suggests that the pyrolysis of [(quinuclidine)GaH$_3$] to give Ga$^0$ is suppressed in the presence of $H_2$. Quite similar to the reaction of [{Cu(mesityl)}$_5$] with [(Me$_3$N)AlH$_3$] as discussed above, the treatment of a mesitylene solution of the same Cu precursor with a solution of [(quinuclidine)GaH$_3$] in mesitylene immediately led to a reaction (Scheme 3) resulting in a dark-red solution. The mixture was stirred under an atmosphere of argon at 150 °C for 24 h and a gray solid formed. The supernatant was decanted, and the gray residue was washed with *n*-pentane and dried.

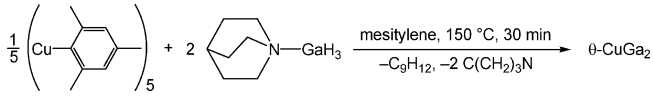


Scheme 3. Synthesis of the intermetallic $\theta$-CuGa$_2$ phase from [{Cu(mesityl)}$_5$] and [(quinuclidine)GaH$_3$].

The X-ray diffraction pattern of the isolated powder reveals all the reflections of the $\theta$-CuGa$_2$ phase (tetragonal *P*4/*mmm*, Figure 6), and it perfectly matches that in the database (JCPDS No. 25-0275). Other phases, as well as metallic Cu or Ga, could not be detected by XRD. Elemental analysis revealed a Cu/Ga ratio of 1:2.08, which is confirmed by EDX. Thus, this reaction offers an approach to a low-temperature CuGa$_2$ phase, which is thermally only stable up to ca. 250 °C. Interestingly, this phase cannot be accessed by conventional metallurgic melting of the two metals, and it is so far only available by mechanical milling of the metal powders.[40] The reaction was also performed in a pressure-stable NMR tube under an atmosphere of argon in order to characterize the organic byproducts. Thus, the precursors were dissolved in [D$_{12}$]mesitylene. Shortly after, a gray solid precipitated. The reaction mixture was heated at 150 °C for 1 h to ensure that the reaction was

  

complete. In the $^1H$ NMR spectrum, the signals of [{Cu(mesityl)}$_5$] were not observed. The hydrogen atoms of the free quinuclidine ligand are found at $\delta$ = 2.75 [m, 6 H, N(C$H_2$)$_3$], 1.54 [sept., 1 H, $H$C(CH$_2$CH$_3$)N], and 1.36 ppm [m, 6 H, HC(C$H_2$CH$_3$)N]. In addition, a singlet at $\delta$ = 4.61 ppm for free $H_2$ was also noted, which is indicative of complete decomposition of the Ga complex. In comparison, the $^1H$ NMR spectral signals of the quinuclidine ligand in [(quinuclidine)GaH$_3$] (in [D$_{12}$]mesitylene) appear at $\delta$ = 2.50, 1.24, and 1.05 ppm, and the signal of the gallium hydrides at $\delta$ = 4.51 ppm.

### Attempts to Obtain a Phase-Pure $Cu_{0.50}Al_{0.50}$ Material

Whereas the formation of the clearly defined $\theta$-$CuAl_2$ phase does not compete with the formation of closely neighboring Cu–Al phases, the synthesis of phase-pure Cu-rich intermetallic Cu–Al phases, which do not exhibit Cu *fcc* structure, is quite an ambitious goal. As mentioned above, the narrow range between 20 and 50 at.-% Al contains numerous phases in which each possesses a unique crystal structure, for example, $\eta_{1,2}$-CuAl, $\zeta_{1,2}$-$Cu_4Al_3$, δ-$Cu_3Al_2$, γ-$Cu_2Al_1$, γ-$Cu_9Al_4$, and β′-$Cu_3Al$. The α-Cu structure appears below 20 at.-% Al.[20] Therefore, the kinetics of the formation of one single phase plays an important role and is intrinsically difficult to control. In this case, a slight deviation of the metal content owing to the introduction of impurities in the organometallic precursors or errors in weighing and quantitative transfer of the rather small quantities of precursors could have a strong effect on the product distribution.

The cohydrogenolysis of a mesitylene suspension of equimolar amounts of [CpCu(PMe$_3$)] and [(Me$_3$N)AlH$_3$] afforded a gray powder upon workup of the reaction mixture. The X-ray powder diffractogram exhibits reflections that could not be assigned to the target $Cu_{0.50}Al_{0.50}$ phase (Figure 7b), but rather to γ-$Cu_9Al_4$ (JCPDS No. 24-0003) together with several Cu-rich phases possibly including γ-$Cu_{6.1}Al_{3.9}$ (JCPDS No. 19-0010). Similar observations were made when [CpCu(PMe$_3$)] and [(AlCp*)$_4$] were used as precursors (Figure 7a). However, there still are several weak reflections at $2\theta$ = 29.83, 32.37, 52.96, and 58.86°, which cannot be indexed as a known phase or as any other likely metallic or oxide material. This suggests the presence of other, presumably poorly crystalline phases that could be Al rich, as only Cu-rich phases were detected by XRD. Subsequently, we substituted [CpCu(PMe$_3$)] by [{Cu(mesityl)}$_5$]. Hence, mesitylene solutions of [{Cu(mesityl)}$_5$] and [(Me$_3$N)AlH$_3$] (5 equiv.; Cu/Al 1:1) were combined in a Fischer–Porter bottle, and a deep-red solution formed. Subsequent treatment with 3 bar $H_2$ at 150 °C afforded a gray precipitate within 15 min. The X-ray diffraction pattern of the obtained powder (Figure 7c) exhibits very broad reflections with low intensity, which could be assigned to the $Cu_{0.51}Al_{0.49}$ phase (monoclinic *C*2/*m*, JCPDS No. 26-0016). The broad line widths of the reflections are also indicative of the presence of other amorphous or nanocrystalline phases in the product. Therefore, the capillary containing the sample was annealed at 200 °C, a temperature at which a material with a bulk melting point of around 650 °C could be considered to crystallize (see Cu–Al phase diagram[4]). Yet, this heat treatment did not lead to crystallization of the sample. Neither the appearance of new reflections nor the sharpening of the observed reflections took place (Figure 7d), presumably as a consequence of an alumina layer covering the particles, which thus prevents agglomeration. Thus, a sample of the powder in a quartz ampoule that was evacuated ($10^{-3}$ mbar), sealed, and subsequently annealed at 500 °C for 24 h exhibits a XRD pattern that could be assigned to the γ-$Cu_9Al_4$ phase (Figure 7e). The reflections assigned to the $Cu_{0.51}Al_{0.49}$ phase are no longer visible in the pattern of the annealed sample.

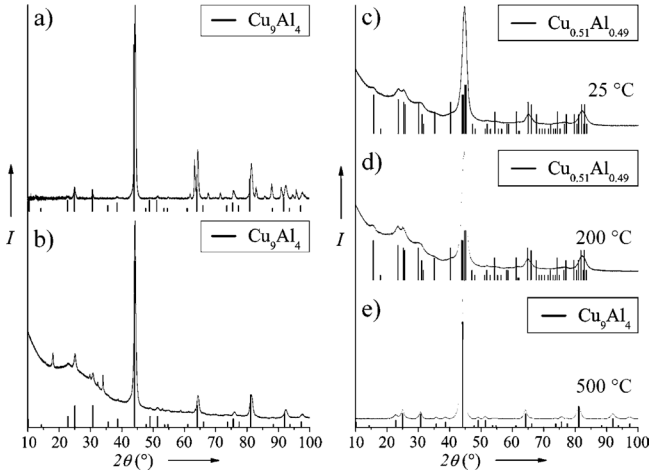


Figure 7. XRD diagrams of the powders obtained by cohydrogenolysis of (a) [CpCu(PMe$_3$)] and 1 equiv. [AlCp*], (b) [CpCu(PMe$_3$)] and 1 equiv. [(Me$_3$N)AlH$_3$], (c) [{Cu(mesityl)}$_5$] and 5 equiv. [(Me$_3$N)AlH$_3$], (d) sample (c) annealed at 200 °C and (e) sample (c) annealed at 500 °C.

The reason for this change is unclear so far. Presumably, a phase transformation took place to give the γ-$Cu_9Al_4$ phase in addition to another Al-rich phase that is not crystalline and, therefore, not observable by XRD. However, we cannot rule out either the presence of more than one phase or the oxidation of the Al component to amorphous $Al_2O_3$ before annealing the powder sample. The $^{27}Al$ MAS NMR spectrum of the as-synthesized material, tentatively denoted as the $Cu_{0.51}Al_{0.49}$ phase, reveals a weak and very broad signal at $\delta$ = 645 ppm and a signal of $Al_2O_3$ at $\delta$ = 21 ppm (see Supporting Information). With decreasing Al concentration, the Knight shift moves to higher field. Below a certain Al content in the alloy, for example, for α-CuAl phases, the Al resonances are generally very difficult to detect without sophisticated NMR spectroscopic techniques. In addition, the XRD data of the sample show that the crystallinity is poor and the obtained phase purity is questionable, as discussed above. Nevertheless we assign the observed signal at $\delta$ = 645 ppm to the Knight shift of Al pointing to a Cu/Al alloyed material in accordance with the XRD data.

  

### Attempted Formation of the γ-$Cu_9Al_4$ Phase

The product of the cohydrogenolysis of [$(Me_3N)AlH_3$] and [$CpCu(PMe_3)$] in a Cu/Al ratio of 9:4 showed α-Cu reflections (shifted Cu reflection due to lattice distortion caused by Al atoms) at $2\theta$ = 42.93 (111), 49.92 (200), 73.34 (220), 88.87 (311), and 93.92° (222). This is similar to the cohydrogenolysis of [$CpCu(PMe_3)$] and [$(AlCp^*)_4$] in the same Cu/Al ratio of 9:4 (see Supporting Information). The Knight shift of Al cannot be observed in these samples. Thus, it can be concluded that it is not possible to selectively synthesize the γ-$Cu_9Al_4$ phase from these precursor combinations under the conditions described. The cohydrogenolysis of [$\{Cu(mesityl)\}_5$] (1 equiv.) and [$(Me_3N)AlH_3$] (2.25 equiv.; molar ratio 2.25:1 = 9:4) afforded a gray powder. Elemental analysis (AAS) of the powder revealed a Cu/Al ratio of 2.15:1.00 = 8.6:4. Similar to the attempted synthesis of the $Cu_{0.51}Al_{0.49}$ material described in the previous section, only $NMe_3$ is found in the supernatant by NMR spectroscopy. The $^{27}Al$ MAS NMR does not show any resonances other than alumina at $\delta$ = 31 ppm with its rotational side bands (Supporting Information). There are no reports in the literature on the Al Knight shift in the γ-$Cu_9Al_4$ alloy that would allow comparisons. According to the XRD pattern in Figure 8a, the sample clearly shows reflections of the targeted γ-$Cu_9Al_4$ phase. However, the reflections are very broad and weak. Therefore, the sealed capillary containing the powder sample was annealed at 200 °C for 24 h. The XRD diagram does not exhibit any change in the diffraction pattern (Figure 8b). After further annealing at 500 °C for 24 h, the XRD pattern changes drastically (Figure 8c). Surprisingly, the initial pattern disappears completely and a set of very sharp reflections develop, which is quite in contrast to the annealing of the $Cu_{0.51}Al_{0.49}$ sample described above (Figure 7). We have so far not been able to identify/assign the Cu–Al phase or any other likely material (such as oxides) for this annealed sample.

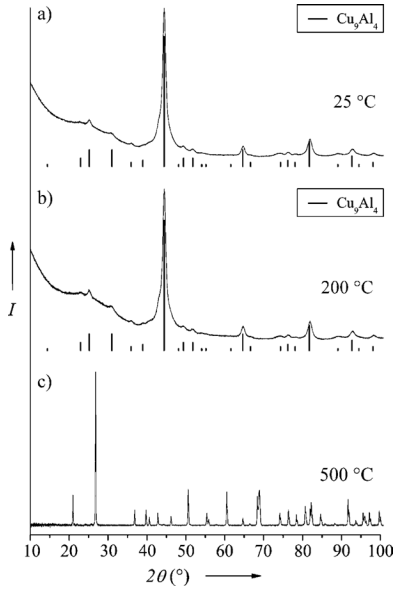


Figure 8. XRD diagrams of (a) 1 equiv. [$\{Cu(mesityl)\}_5$] and 2.2 equiv. [$(Me_3N)AlH_3$], (b) the powder of (a) annealed at 200 °C, and (c) the powder of (a) annealed at 500 °C.

### Reactions in the Presence of Surfactants

The treatment of solutions of [$CpCu(PMe_3)$] or [$\{Cu(mesityl)\}_5$] with solutions of [$(Me_3N)AlH_3$] in the presence of the surfactant poly(2,6-dimethyl)(1,4-phenylene oxide) (PPO) resulted in the formation of precipitates rather than colloids. Irrespective of the way the two reagents were mixed, we found no effect on the particle growth and agglomeration. Addition of HDA to a mesitylene solution of the Cu precursors followed by slow addition of [$(Me_3N)AlH_3$] also did not prevent precipitation of the particles, even at –50 °C. Thus, our attempts to prepare colloidal intermetallic Cu/Al nanoparticles by using [$(Me_3N)AlH_3$] as the Al source instead of [$(AlCp^*)_4$] and PPO or HDA as stabilizing agents failed possibly due to the extreme reactivity of the Al precursor, as we have suggested in our previous publication of copper aluminum alloy colloids.[22a]

## Conclusions

In summary, it was shown that the Al complex [$(Me_3N)AlH_3$] is a valuable precursor for the synthesis of nanoscale copper aluminum alloys. The alane offers several advantages over the $Al^I$ compound [$(AlCp^*)_4$]. Whereas [$(Me_3N)AlH_3$] can easily be synthesized in mass scales of 20 g by a simple salt metathesis reaction from $Me_3NHCl$ and $LiAlH_4$,[41] the low-valent $Al^I$ compound is synthesized in four reaction steps, including the synthetically delicate reduction of $Al^{III}$ to $Al^I$ by the Na/K alloy.[42] However, in contrast, the alane is highly reactive and the reactions are very vigorous and less controlled. Attempts to prepare a colloidal solution of Al nanoparticles by using either [$(Me_3N)AlH_3$] or [$(AlCp^*)_4$] failed. The [$(AlCp^*)_4$] compound is a mild reagent, which first has to be dissolved in a solvent before it decomposes to $Al^0$. This causes an intrinsic delay of decomposition, so that the time scale of releasing $Al^0$ matches quite well with that of the metal precursors used herein. Although the cohydrogenolysis of [$CpCu(PMe_3)$] with both [$(AlCp^*)_4$] and [$(Me_3N)AlH_3$] gives the apparently pure $\theta$-$CuAl_2$ phase, the products are contaminated with, thus far, an unidentified phosphane-based side product, which is quite difficult to remove. With [$CpCu(PMe_3)$], it was also not possible to obtain other Cu-rich α-CuAl phases in the same quality of phase purity. The compound [$\{Cu(mesityl)\}_5$] instead is a very clean source of $Cu^0$ upon hydrogenolysis in mesitylene solution. In contrast to the Cu–phosphane complex, it reacts with [$(Me_3N)AlH_3$] to give obviously phase-pure $\theta$-$CuAl_2$. In addition, the synthesis of copper-rich phases such as $Cu_{0.50}Al_{0.50}$ and γ-$Cu_9Al_4$ were investigated; however, it could not be unambiguously excluded that other phases are present. The phase selectivity of the soft-chemical approach remains questionable in these cases. Although scale up of the synthesis of

  

the organometallic precursors is certainly possible, which thus enables scale up of the soft-chemical synthesis, the value of the above-outlined soft-chemical approach is certainly not to compete with established metallurgical processes. Rather, the synthesis of the low-temperature θ-$CuGa_2$ phase (decomposition above 250 °C) that was formed by the reaction of [{Cu(mesityl)}$_5$] and [(quinuclidine)$GaH_3$] nicely demonstrates the potential of the presented precursor concept, namely, the access to metastable alloy phases, which are less accessible by traditional metallurgical routes.

## Experimental Section

**General Considerations:** All manipulations and chemical reactions were conducted by using Schlenk lines and glove box techniques (Ar, $H_2O$, $O_2$ <1 ppm) and sealed Fischer–Porter vessels (Andrews Glass, volume: 90 mL). Solvents were dried by passing through a pad of activated alumina (chromatography grade, Merck) on a Schlenk frit and subsequently distilled. [$D_{12}$]Mesitylene (Deutero GmbH) was dried with activated molecular sieves and degassed by several freeze–pump–thaw cycles. All other solvents (purchased by Merck) used were dried, degassed, and saturated with argon by using a continuous solvent purification system (MBraun; $H_2O$ content below 1 ppm). All powder X-ray diffractograms were recorded with a D8-Advance-Bruker-AXS diffractometer (Cu-$K_\alpha$ radiation) in θ–2θ-geometry and a position sensitive detector (capillary technique under argon, thickness: 0.7 mm). TEM measurements were carried out with a Hitachi-H-8100 instrument (Accelerating voltage up to 200 kV, $LaB_6$ filament). The TEM samples were prepared from diluted solutions or suspensions in toluene on carbon-coated gold grids (Plano). The NMR spectra in solution were obtained by using a Bruker DPX 250 MHz or DRX 400 MHz spectrometer in $C_6H_6$, $C_6D_6$, or [$D_{12}$]mesitylene ($T$ = 25 °C, $^1$H: 250.1 MHz, $^{27}$Al: 65.2 MHz). The chemical shifts (in δ ppm) are referenced to the residual proton signals of the deuterated solvent ($C_6D_6$: $^1$H 7.15 ppm; [$D_{12}$]mesitylene: $^1$H 6.67 and 2.16 ppm) or the probe head {$^{27}$Al: 68 ppm, referenced to $[Al(H_2O)_6]^{3+}$ set at 0 ppm}. Small-scale hydrogenolysis reactions were carried out in pressure-stable NMR tubes fitted with PTFE screw caps (Wilmad-LabGlass). Solid-state $^{27}$Al MAS NMR spectral measurements were carried out with a Bruker DSX 400 MHz spectrometer, with a rotation frequency of 20 kHz ($T$ = 25 °C, 104.2 MHz). Gas chromatographic–mass spectral measurements were performed with a Shimadzu GCMS-QP2010. Elemental analyses were obtained by using Elementar Vario III atomic absorption spectrometer (AAS). The compounds [{Cu(mesityl)$_5$}],[32] [CpCu($PMe_3$)],[43] [(quinuclidine)$GaH_3$],[44] and [$(AlCp^*)_4$][42] were synthesized according to literature reports. [$(Me_3N)AlH_3$] was prepared by a modification of the procedure published by Jouet et al.[41] from $Me_3NHCl$ (Aldrich) and $LiAlH_4$ (Acros) in toluene, and the product was purified by crystallization from a saturated toluene solution.

**Hydrogenolysis of [{Cu(mesityl)}$_5$] to Yield Cu:** A yellow solution of [{Cu(mesityl)}$_5$] (0.100 g, 0.547 mmol) in mesitylene (10 mL) was treated with $H_2$ (3 bar) in a Fischer–Porter bottle and heated at 150 °C. After 15 min, a red-brown, metallic shiny solid formed. The reaction was stirred for 1 h. Thereafter, the reaction was worked up as described above. Yield: 0.031 g (89%). AAS: 99 wt.-% Cu. XRD reflections (2θ): 43.30 (111), 50.48 (200), 74.14 (220), 90.06 (311), 95.21° (222).

**Hydrogenolysis of [$(Me_3N)AlH_3$] to Al Powder:** In a Fischer–Porter bottle, [$(Me_3N)AlH_3$] (0.100 g, 1.122 mmol) was dissolved in mesitylene (10 mL). This solution was degassed in vacuo; the bottle was then pressurized with $H_2$ (3 bar) and placed into a 150 °C hot oil bath. After 1 h, a gray precipitate formed, which was allowed to settle in the glove box. The colorless supernatant was carefully removed with a syringe. The residue was washed with *n*-pentane (3 × 20 mL) and dried in vacuo ($10^{-3}$ mbar) Yield: 0.026 g (86%). AAS: 99.7 wt.-% Al. $^{27}$Al MAS NMR (104.2 MHz, 25 °C, $\nu$ = 20 KHz): $\delta$ = 1640 ($Al^0$), 56 ($AlO_4$), 1 ($AlO_6$) ppm. XRD reflections (2θ): 38.53 (111), 44.81 (200), 65.25 (220), 78.36 (311), 82.58 (222)°.

This reaction was also performed in a pressure-stable NMR tube: [$(Me_3N)AlH_3$] (0.010 g, 0.112 mmol) was dissolved in [$D_{12}$]mesitylene (0.7 mL), and the tube was then pressurized with $H_2$ (3 bar) and heated to 150 °C. After 5 min, $Al^0$ precipitated. NMR spectra were recorded after 1 h at 150 °C. $^1$H NMR (250.1 MHz, 25 °C): $\delta$ = 2.11 [s, 9 H, $N(CH_3)_3$] ppm.

**Reaction of [CpCu($PMe_3$)] with [$(Me_3N)AlH_3$]:** In a Fischer–Porter bottle, [CpCu($PMe_3$)] (0.224 g, 1.094 mmol) and a stoichiometric amount of [$(Me_3N)AlH_3$] were dissolved in mesitylene (20 mL). The required masses of Al precursor for targeting the respective Cu–Al phases are given in Table 1. The precursors reacted immediately, whereupon a gray solid formed. In order to ensure completion of the reaction, the bottle was set to 3 bar $H_2$ pressure and placed in a 150 °C hot oil bath and stirred for 24 h. The residue was washed with hot 1,4-dioxane (3 × 20 mL) to remove the P-containing byproduct and then washed with *n*-pentane (3 × 20 mL). Subsequently, the gray powder was dried in vacuo ($10^{-3}$ mbar). The yields are listed in Table 1. EDX ($x$ = 0.67): 30 at.-% Cu, 70 at.-% Al. $^{27}$Al MAS NMR (104.2 MHz, 25 °C, $\nu$ = 20 KHz): $\delta$ = 1492 ($Al^0$), 31 ($Al_2O_3$) ppm. XRD data are given in the Supporting Information.

Table 1. Required masses of [$(Me_3N)AlH_3$] for the formation of $Cu_{1-x}Al_x$ phases.

| $Cu_{1-x}Al_x$ | $m$([$(Me_3N)AlH_3$]) | Elemental analysis [%] | Cu/Al ratio and sum formula | Yield |
|---|---|---|---|---|
| $x$ = 0.67 | 0.195 g (2.819 mmol) | Cu 42.7 Al 38.6 | 1.00:2.12 ($Cu_{0.32}Al_{0.68}$) | 0.103 g (80%) |
| $x$ = 0.50 | 0.098 g (1.095 mmol) | Cu 50.9 Al 23.1 | 1.00:1.07 ($Cu_{0.48}Al_{0.52}$) | 0.072 g (73%) |
| $x$ = 0.31 | 0.043 g (0.482 mmol) | Cu 64.4 Al 12.5 | 1.00:0.46 ($Cu_{0.68}Al_{0.32}$) | 0.058 g (70%) |

This reaction was also performed in a pressure-stable NMR tube: [CpCu($PMe_3$)] (0.010 g, 0.049 mmol) and [$(Me_3N)AlH_3$] (0.0087 g, 0.098 mmol) were dissolved in [$D_{12}$]mesitylene (0.7 mL), and the tube was then pressurized with 4 bar $H_2$ and heated to 150 °C. After 5 min, θ-$CuAl_2$ precipitated. NMR spectra were recorded after 24 h at 150 °C. $^1$H NMR (250.1 MHz, 25 °C): $\delta$ = 6.49 (m, 2 H, CpH, *meta-H*), 6.32 (m, 2 H, CpH, *ortho-H*), 2.75 (m, 2 H, *ipso*-H), 2.11 [s, 9 H, $N(CH_3)_3$], 0.82 [d, $^2J_{P,H}$ = 2.634 Hz, 9 H, $P(CH_3)_3$] ppm.

**Reactions of [{Cu(mesityl)$_5$}] with [$(Me_3N)AlH_3$]:** To a solution of [{Cu(mesityl)}$_5$] (0.200 g, 1.094 mmol) in mesitylene (10 mL) in a Fischer–Porter bottle was added by syringe a solution of [$(Me_3N)$-$AlH_3$] in mesitylene (10 mL), whereupon the color of the solution in all the cases turned dark red. The required masses for the respective $Cu_{1-x}Al_x$ phase are given in Table 2. The solution was degassed, set to 3 bar $H_2$, and heated for 3 d at 150 °C, whereupon a gray, metallic solid precipitated. The colorless supernatant and the residue were separated as described above. The yields are given in

  

Table 2. EDX ($x$ = 0.67): 33 at.-% Cu, 67 at.-% Al. $^{27}$Al MAS NMR (104.2 MHz, 25 °C, $\nu$ = 20 KHz): $\delta$ = 1495 ($Al^0$) ppm. XRD data are listed in the Supporting Information.

Table 2. Required masses of $[(Me_3N)AlH_3]$ for the formation of the $Cu_{1-x}Al_x$ phases.

| $Cu_{1-x}Al_x$ | $m([(Me_3N)AlH_3])$ | Elemental analysis [%] | Cu/Al ratio and sum formula | Yield |
|---|---|---|---|---|
| $x$ = 0.67 | 0.195 g (2.819 mmol) | Cu 46.9 Al 42.0 | 1.00:2.11 ($Cu_{0.32}Al_{0.68}$) | 0.113 g (88%) |
| $x$ = 0.50 | 0.098 g (1.095 mmol) | Cu 57.8 Al 22.3 | 1:00:0.91 ($Cu_{0.52}Al_{0.48}$) | 0.086 g (87%) |
| $x$ = 0.31 | 0.043 g (0.482 mmol) | Cu 70.3 Al 13.4 | 1.00:0.45 ($Cu_{0.69}Al_{0.31}$) | 0.076 g (92%) |

Data for $x$ = 0.50: $^{27}$Al MAS NMR (104.2 MHz, 25 °C, $\nu$ = 20 KHz): $\delta$ = 645 ($Al^0$), 21 ($Al_2O_3$). XRD reflections (2$\theta$): 15.61 (001), 23.55 (–110), 25.20 (–111), 30.89 (–311), 44.62 (–511), 63.97 (–622), 76.69 (800), 82.12° (–333). Data for $x$ = 0.31. XRD reflections (2$\theta$): 22.72 (210), 25.08 (211), 30.66 (300), 35.85 (222), 44.14 (330), 49.00 (332), 51.36 (422), 64.26 (600), 73.61 (631), 75.74 (444), 77.64 (550), 81.29 (721), 88.40 (651), 92.06 (741), 97.50° (660).

For $x$ = 0.67 ($\theta$-$CuAl_2$), this reaction was also performed in a pressure-stable NMR tube: $[\{Cu(mesityl)\}_5]$ (0.010 g, 0.055 mmol) and $[(Me_3N)AlH_3]$ (0.0098 g, 0.110 mmol) were dissolved in $[D_{12}]$mesitylene (0.7 mL), and the tube was then pressurized with 4 bar $H_2$ and heated to 150 °C. After 5 min, $\theta$-$CuAl_2$ precipitated. NMR spectra were recorded after 24 h at 150 °C. $^1$H NMR (250.1 MHz, 25 °C): $\delta$ = 2.11 [s, 9 H, $N(CH_3)_3$] ppm.

**Synthesis of the $\theta$-$CuGa_2$ Phase:** Samples of $[\{Cu(mesityl)\}_5]$ (0.050 g, 0.273 mmol) and $[(quinuclidine)GaH_3]$ (0.100 g, 0.547 mmol) were combined in a Fischer–Porter bottle. When the two solids were shaken together, the colorless-to-pale-yellow mixture turned slightly brownish black indicating an apparent reaction. Addition of mesitylene (10 mL) to this mixture resulted in a reddish brown homogeneous solution with vigorous gas evolution. The bottle was placed in an oil bath at 150 °C and within 5–10 min, a black solid precipitated. After 4 h of heating, the solution was cooled, the supernatant was carefully decanted, and the black precipitate was washed with $n$-pentane (3 × 20 mL) and dried in vacuo. Yield: 0.047 g (87%). XRD reflections (2$\theta$): 15.14 (001), 30.62 (002), 31.54 (100), 35.17 (101), 44.54 (102), 45.25 (110), 46.67 (003), 47.98 (111), 55.65 (112), 57.49 (103), 63.78 (004), 65.98 (200), 67.06 (113), 68.14 (102), 72.94 (104), 74.47 (202), 75.01 (210), 77.04 (211). AAS: 23.3 wt.-% Cu, 53.3 wt.-% Ga.

The reaction was repeated in a pressure-stable NMR tube: $[\{Cu(mesityl)\}_5]$ (0.010 g, 0.055 mmol) and $[(quinuclidine)GaH_3]$ (0.020 g, 0.110 mmol) were dissolved in $[D_{12}]$mesitylene (0.7 mL). After 5 min, $\theta$-$CuGa_2$ precipitated. In order to ensure completion of the reaction, the mixture was heated to 150 °C for 1 h. $^1$H NMR (250.1 MHz, 25 °C): $\delta$ = 4.61 ($H_2$), 2.75 [m, 6 H, $HC(CH_2CH_2)_3N$], 1.54 [sept., 1 H, $HC(CH_2CH_2)_3N$], 1.36 [m, 6 H, $HC(CH_2CH_2)_3N$].

**Supporting Information** (see footnote on the first page of this article): General synthesis procedure for $Cu_{1-x}Al_x$ by hydrogenolysis of $[CpCu(PMe_3)]$ and $[(AlCp^*)_4]$; XRD reflections of the synthesized $\theta$-$CuAl_2$ phases; $^1$H and $^{27}$Al NMR spectra of $[(Me_3N)AlH_3]$ before and after hydrogenolysis; $^{27}$Al MAS NMR spectra of the obtained Al powder and that of $\theta$-$CuAl_2$ synthesized by cohydrogenolysis of $[(Me_3N)AlH_3]$ with $[CpCu(PMe_3)]$ and $[\{Cu(mesityl)\}_5]$, respectively; $^1$H NMR spectra of the hydrogenolysis of $[\{Cu(mesityl)\}_5]$, XRD diagrams of $\theta$-$CuAl_2$ from hydrogenolysis of $[CpCu(PMe_3)]$ and 0.5 equiv. $[(AlCp^*)_4]$ before and after workup; XRD diagram of α-Cu from hydrogenolysis of 9 equiv. $[CpCu(PMe_3)]$ and 4 equiv. $[(AlCp^*)_4]$.

## Acknowledgments

B. R. J. thanks the Alexander-von-Humboldt Foundation for a fellowship and the German Research Foundation (DFG) for support within the Research Centre SFB 558 "Metal Support Interaction in Heterogeneous Catalysis".

[1] a) E. G. West in *Copper and Its Alloys* (Ed.: E. Harwood), Chichester, **1982**; b) J. Behm, T. Priermeier, W. Scherer, R. A. Fischer, *Angew. Chem. Int. Ed. Engl.* **1993**, *32*, 746–748; c) R. A. Fischer, T. Priermeier, *Organometallics* **1994**, *13*, 4306–4314; d) R. A. Fischer, A. Miehr, M. M. Schulte, *Adv. Mater.* **1995**, *7*, 58–61; e) R. A. Fischer, A. Miehr, T. Metzger, E. Born, O. Ambacher, R. Dimitrov, *Chem. Mater.* **1996**, *8*, 1356–1359; f) R. A. Fischer, A. Miehr, *Chem. Mater.* **1996**, *8*, 497–508.
[2] G. Trambly de Laissardière, D. Nguyen-Manh, D. Mayou, *Prog. Mater. Sci.* **2005**, *50*, 679–788.
[3] a) Guinier, *Nature* **1938**, *142*, 569–570; b) G. D. Preston, *Nature* **1938**, *142*, 570; c) G. D. Preston, *Proc. R. Soc. London Ser. A* **1938**, *167*, 526–538; d) G. D. Preston, *Phil. Magn.* **1938**, *26*, 855–871; e) J. M. Silcock, T. Heal, H. K. Hardy, *J. Inst. Met.* **1954**, *82*, 239–248; f) D. J. Stockdale, *Inst. Met.* **1933**, *52*, 111–117; g) T. Gödecke, F. Sommer, *Z. Metallkd.* **1996**, *87*, 581–586.
[4] a) M. Hansen (Ed.), *Constitution of Binary Alloys*, 2nd ed., McGraw–Hill, New York, **1958**; b) J. L. Murray, *Int. Met. Rev.* **1985**, *30*, 211–233.
[5] E. E. Havinga, H. Damsma, P. Hokkeling, *J. Less-Common Met.* **1972**, *27*, 169–186.
[6] Y. Grin, F. R. Wagner, M. Armbrüster, M. Kohout, A. Leithe-Jasper, U. Schwarz, U. Wedig, H. G. von Schnering, *J. Solid State Chem.* **2006**, *179*, 1707–1719.
[7] F. Haarmann, M. Armbrüster, Y. Grin, *Chem. Mater.* **2007**, *19*, 1147–1153.
[8] M. El-Boragy, R. Szepan, K. Schubert, *J. Less-Common Met.* **1972**, *29*, 133–140.
[9] L. D. Gulay, B. Harbrecht, *J. Alloys Compd.* **2004**, *367*, 103–108.
[10] L. D. Gulay, B. Harbrecht, *Z. Allg. Anorg. Chem.* **2003**, *629*, 463–466.
[11] S. Xi, J. Zhou, D. Zhang, X. Wang, *Mater. Lett.* **1996**, *26*, 245–248.
[12] J. C. de Lima, D. M. de Trichês, V. H. F. dos Santos, T. A. J. Grandi, *J. Alloys Compd.* **1999**, *282*, 258–260.
[13] M. Abbasi, A. K. Taheri, M. T. Salehi, *J. Alloys Compd.* **2001**, *319*, 233–241.
[14] D. Y. Ying, D. L. Zhang, *J. Alloys Compd.* **2000**, *311*, 275–282.
[15] S. Xi, X. Qu, M. Ma, J. Zhou, X. Zheng, X. Wang, *J. Alloys Compd.* **1998**, *268*, 211–214.
[16] X. J. Peng, R. Wuhrer, G. Heness, W. Y. Yeung, *J. Mater. Sci.* **1999**, *34*, 2029–2038.
[17] L. Dubourg, H. Pelletier, D. Vaissiere, F. Hlawka, A. Cornet, *Wear* **2002**, *253*, 1077–1085.
[18] H. G. Jiang, J. Y. Dai, H. Y. Tong, B. Z. Ding, Q. H. Song, Z. Q. Hu, *J. Appl. Phys.* **1993**, *74*, 6165–6169.
[19] a) M. van Sande, J. Van Landuyt, M. Avalos-Borja, G. Torres Villaseñor, S. Amelinckx, *Mater. Sci. Eng.* **1980**, *46*, 167–173; b) Y. Koyama, M. Hatano, M. Tanimura, *Phys. Rev. B* **1996**, *53*, 11462–11468.
[20] a) M.-A. Nicolet, S. S. Lau in *VLSI Electronics Microstructure Science* (Eds.: N. G. Einspruch, G. B. Larrabee), Academic, New York, **1983**; b) W. L. Johnson, *Prog. Mater. Sci.* **1986**, *30*, 81–134.

  

[21] See recent reviews: a) A.-H. Lu, E. L. Salabas, F. Schüth, *Angew. Chem. Int. Ed.* **2007**, *46*, 1222–1244; b) Y.-W. Jun, J.-S. Choi, J. Cheon, *Chem. Commun.* **2007**, 1203–1214; c) S. Sun, *Adv. Mater.* **2006**, *18*, 393–403; d) M. Green, *Chem. Commun.* **2005**, 3002–3011; e) B. L. Cushing, V. L. Kolesnichenko, C. J. O'Connor, *Chem. Rev.* **2004**, *104*, 3893–3946; f) N. Toshima, T. Yonezawa, *New J. Chem.* **1998**, *22*, 1179–1201.
[22] a) M. Cokoja, H. Parala, M. K. Schröter, A. Birkner, M. W. E. van den Berg, W. Grünert, R. A. Fischer, *Chem. Mater.* **2006**, *18*, 1634–1642; b) M. Cokoja, H. Parala, M.-K. Schröter, M. W. E. van den Berg, K. V. Klementiev, W. Grünert, R. A. Fischer, *J. Mater. Chem.* **2006**, *16*, 2420–2428.
[23] M.-K. Schröter, L. Khodeir, M. W. E. van den Berg, T. Hikov, M. Cokoja, S. Miao, W. Grünert, M. Muhler, R. A. Fischer, *Chem. Commun.* **2006**, 2498–2500.
[24] a) J. Hambrock, R. Becker, A. Birkner, J. Weiß, R. A. Fischer, *Chem. Commun.* **2002**, 68–69; b) R. Becker, J. Weiß, A. Devi, R. A. Fischer, *J. Phys. IV* **2001**, *11*, 569–575.
[25] W. L. Gladfelter, D. C. Boyd, K. F. Jensen, *Chem. Mater.* **1989**, *1*, 339–343.
[26] a) J. A. Haber, P. C. Gibbons, W. E. Buhro, *J. Am. Chem. Soc.* **1997**, *119*, 5455–5456; b) J. A. Haber, W. E. Buhro, *J. Am. Chem. Soc.* **1998**, *120*, 10847–10855; c) K. T. Higa, C. E. Johnson, R. A. Hollins, U. S. Patent, 5,885,321, **1999**.
[27] B. Bogdanović, K.-H. Claus, S. Gürtzgen, B. Spliethoff, U. Wilczok, *J. Less-Common Met.* **1987**, *131*, 163–172.
[28] a) W. E. Buhro, J. A. Haber, B. E. Waller, T. J. Trentler, R. Suryanarayanan, C. A. Frey, S. M. L. Sastry, *Polym. Mater. Sci. Eng.* **1995**, *73*, 39–40; b) J. A. Haber, N. V. Gunda, W. E. Buhro, *J. Aerosol Sci.* **1998**, *29*, 637–645; c) J. A. Haber, N. V. Gunda, J. J. Balbach, M. S. Conradi, W. E. Buhro, *Chem. Mater.* **2000**, *12*, 973–982.
[29] J. A. Haber, J. L. Crane, W. E. Buhro, C. A. Frey, S. M. L. Sastry, J. J. Balbach, M. S. Conradi, *Adv. Mater.* **1996**, *8*, 163–166.
[30] a) Y. B. Pithawalla, S. Deevi, *Mater. Res. Bull.* **2004**, *39*, 2303–2316; b) D. P. Dutta, G. Sharma, A. K. Rajarajan, S. M. Yusuf, G. K. Dey, *Chem. Mater.* **2007**, *19*, 1221–1225.
[31] M. Cokoja, H. Parala, A. Birkner, O. Shekhah, M. W. E. van den Berg, R. A. Fischer, *Chem. Mater.* **2007**, *19*, 5721–5733.
[32] E. M. Meyer, S. Gambarotta, C. Floriani, A. Chiesi-Villa, C. Guastini, *Organometallics* **1989**, *8*, 1067–1079.
[33] S. D. Bunge, T. J. Boyle, T. J. Headley, *Nano Lett.* **2003**, *3*, 901–905.
[34] a) C. Amiens, B. Chaudret, *Mod. Phys. Lett. B* **2007**, *21*, 1133–1141; b) D. Wostek-Wojciechowska, J. K. Jeszka, C. Amiens, B. Chaudret, P. Lecante, *J. Colloid Interf. Sci.* **2005**, *287*, 107–113; c) B. Chaudret, *Acualité Chimique* **2005**, *290–291*, 33–43; d) B. Chaudret, *CR. Phys.* **2005**, *6*, 117–131; e) K. Philippot, B. Chaudret, *CR. Chim.* **2003**, *6*, 1019–1034; f) F. Dumestre, B. Chaudret, C. Amiens, P. Renaud, P. Fejes, *Science* **2004**, *303*, 821–823.
[35] D. B. Beach, S. E. Blum, F. K. LeGoues, *J. Vac. Sci. Technolog. A* **1989**, *7*, 3117–3118.
[36] a) T. J. Bastow, M. E. Smith, *J. Phys.: Condens. Matter* **1995**, *7*, 4929–4937; b) M. Veith, K. Andres, S. Faber, J. Blin, M. Zimmer, Y. Wolf, H. Schnöckel, R. Köppe, R. de Masi, S. Hüfner, *Eur. J. Inorg. Chem.* **2003**, 4387–4393; c) reference measurements were performed at the Ruhr-University Bochum with Al powder (Fluka) and $Al_2O_3$ (neutral, for column chromatography, Merck). The $Al^0$ signal appeared at $\delta$ = 1640 ppm and the two $Al_2O_3$ signals were found at 68 and 8 ppm.
[37] a) D. Müller, W. Gessner, H.-J. Behrens, G. Scheler, *Chem. Phys. Lett.* **1981**, *79*, 59–62; b) G. Kunath-Fandrei, T. J. Bastow, J. S. Hall, C. Jäger, M. E. Smith, *J. Phys. Chem.* **1995**, *99*, 15138–15141.
[38] T. J. Bastow, S. Celotto, *Acta Mater.* **2003**, *51*, 4621–4630.
[39] D. R. Torgesson, R. G. Barnes, *J. Chem. Phys.* **1975**, *62*, 3968–3973.
[40] a) S.-J. Hong, C. Suryanarayana, *J. Appl. Phys.* **2004**, *96*, 6120–6126; b) K. T. Lee, Y. S. Jung, J. Y. Kwon, J. H. Kim, S. M. Oh, *Chem. Mater.* **2008**, *20*, 447–453.
[41] R. J. Jouet, A. D. Warren, D. M. Rosenberg, V. J. Bellitto, K. Park, M. R. Zachariah, *Chem. Mater.* **2005**, *17*, 2987–2996.
[42] M. Schormann, K. S. Klimek, H. Hatop, S. P. Varkey, H. W. Roesky, C. Lehmann, C. Röpken, R. Herbst-Irmer, M. Noltemeyer, *J. Solid State Chem.* **2001**, *162*, 225–236.
[43] H. Werner, H. Otto, T. Ngo-Khac, C. Burschka, *J. Organomet. Chem.* **1984**, *262*, 123–136.
[44] J. L. Atwood, S. G. Bott, F. M. Elms, C. Jones, C. L. Raston, *Inorg. Chem.* **1991**, *30*, 3792–3793.

Received: January 15, 2008
Published Online: June 18, 2008

  